Investigation of the Structure of Liquid Pyridine: a Molecular Dynamics Simulation, an RISM, and an X-ray Diffraction Study

Imre Bakó, Tamás Radnai, and Gábor Pálinkás

Central Research Institute for Chemistry of the Hungarian Academy of Sciences, Budapest, P.O. Box 17, H-1525 Hungary

Z. Naturforsch. **51a**, 859–866 (1996); received October 20, 1996

The structure of liquid pyridine is investigated by molecular dynamics simulation and the RISM integral equation methods. The calculated total radial distribution functions (RDF) are compared with the experimental RDF's, obtained by X-ray diffraction measurement. It is shown that the local structure of liquid pyridine is mainly determined by the dipole-dipole interaction between the molecules. The local order is characterized by the pair distribution functions, angular correlation functions and orientational distributions. Dynamical properties (self-diffusion coefficients, rotational correlation times and reorientational correlation times) calculated on the basis of MD results are in good agreement with experimental data.

Introduction

Liquid pyridine is a representative of dipolar molecular liquids, composed of planar molecules which, in contrast to the benzene molecules, have a high dipole moment. Authors of several papers on molecular dynamics (MD) and Monte Carlo (MC) computer simulations of liquid benzene [1–6] suggested that the preferred relative orientation of nearest neighbor molecules can be described by a T-shaped configuration, and that the structure of the liquid roughly resembles to that of benzene in the crystalline state. On the other hand, the crystal structure of pyridine is fairly complicated and significantly different from the crystal structure of benzene. It is worth questioning whether or not the differences in the crystal structures of the two compounds are inherited by the structures in the liquid state and what is the role of the dipole-dipole interactions in forming the local order in the liquid. Previous studies on the liquid structure of pyridine are less abundant than those on liquid benzene. Gamba and Klein reported the only study on liquid pyridine by the MD method [7]. Their investigation was confined to a small periodic box, and they did not analyze the structure of the liquid. Bertagnolli et al. performed an X-ray and a neutron diffraction experiment on liquid pyridine and concluded that the dipolar interaction is the structure determining factor [8]. Since, however, no related computer simulation studies were performed, the diffraction studies alone could not result in a detailed structure of the liquid.

In the present work we report some results obtained with a new molecular dynamics simulation. The liquid structure is analyzed in terms of the total radial distribution function, structure function, site-site pair distribution functions and angular correlation functions. The structural data obtained from the MD simulation are compared to those calculated by the RISM integral equation theory and to the results of a newly performed X-ray diffraction experiment. Dynamical data computed on the basis of the MD simulation are also discussed in detail. Some preliminary structural data based upon the present MD simulation had already been published in [9], but no detailed analysis has been reported so far.

1. Methods

1.1 Molecular Dynamics Simulation

The interaction potential of the pyridine molecules was constructed in terms of pair-potentials of OPLS type. A pyridine molecule was represented by six sites, i.e., five equal sites for CH groups and one site for the N atom. The Lennard Jones (12-6) parameters and the charge distribution were taken from Jorgensen et al. [10] (CH: $\sigma = 3.75$ Å, $\varepsilon = 0.46$ kJ/mol, N: $\sigma = 3.25$ Å, $\varepsilon = 0.71$ kJ/mol). The charge distribution in a pyridine

Reprint requests to Dr. G. Pálinkás.

0932-0784 / 96 / 0700-0859 $ 06.00 © – Verlag der Zeitschrift für Naturforschung, D-72072 Tübingen

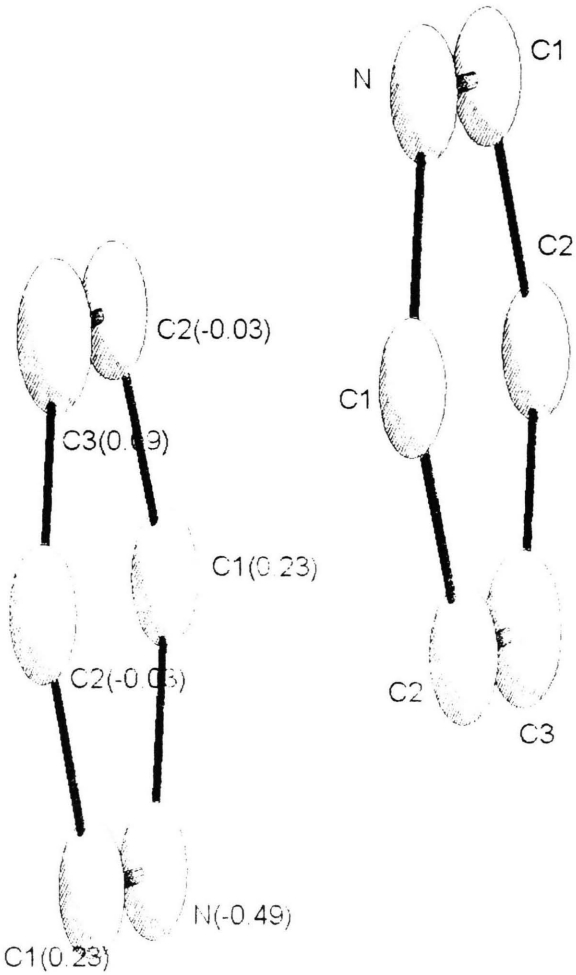

Fig. 1. Optimized structure of a pyridine dimer.

molecule and the optimized structure of an isolated dimer are shown in Figure 1. As can be seen, the two molecules are aligned parallel with their dipole vectors pointing in opposite directions. This alignment, referred to as antidipole orientation hereafter, has often been found as preferred between the neighboring molecules in aprotic, dipolar liquids [9]. The dimerization energy was found to be -15.7 kJ/mol at the minimum energy configuration.

The studied system consisted of 256 pyridine molecules. The periodic cube had a volume in accordance with macroscopic density of 0.978 g/cm^3. The calculation was carried out in the microcanonical ensemble. The simulation program MDMPOL coded by Smith and Fincham [11] was used. The orientation of the molecules was described by the quaternion representation method. The Ewald summation was used for all Coulombic interactions. The simulation run was extended, after complete equilibration, over 15,000 time steps equivalent to a total elapsed time of 30 ps with an average temperature of 295 K without rescaling the velocities. The mean potential energy resulted in -38.5 kJ/mol, which compares well with the experimental heat of evaporation of -40.4 kJ/mol.

1.2 Integral Equation Formulation

The RISM integral equation for a molecular fluid with a molecular number density ϱ and containing m sites per molecule can be written as [12]

$$\varrho c \varrho = \omega c \omega + \varrho \omega c h , \tag{1}$$

where h, c and ω are Fourier transforms of the total, direct, and intramolecular pair correlation functions, respectively.

The selected closure relation was according to a hypernetted chain approximation, which is given by

$$c_{\alpha\gamma} = -\beta U_{\alpha\gamma} + h_{\alpha\gamma} + \ln(g_{\alpha\gamma}) , \tag{2}$$

where $U_{\alpha\beta}$ is the pair potential energy between two sites α, β located on different molecules. The potential set was identical to what was used in the MD simulation. The RISM integral equation was solved numerically by Monson's method [13].

2. Results

2.1 Structure of Liquid Pyridine

2.1.1 Radial Distribution Functions

In order to obtain a detailed structural information about pyridine in the liquid state, we computed several radial distribution functions (RDF), based on the MD simulation and the RISM calculation.

Five computed distribution functions are shown in Figure 2. Four of them are functions of i-C_{all}, where i stands for an atomic site considered in the origin, and C_{all} stands for all carbon atoms at the distance r from the origin. The numbering of the carbon atoms is shown in Figure 1. According to Fig. 2, the MD and RISM results are in a good agreement. All five RDF's show broad first peaks ranging from the closest allowable approach of the atoms near 3 Å to well defined minima near 6–7 Å. Some enhanced order appears for

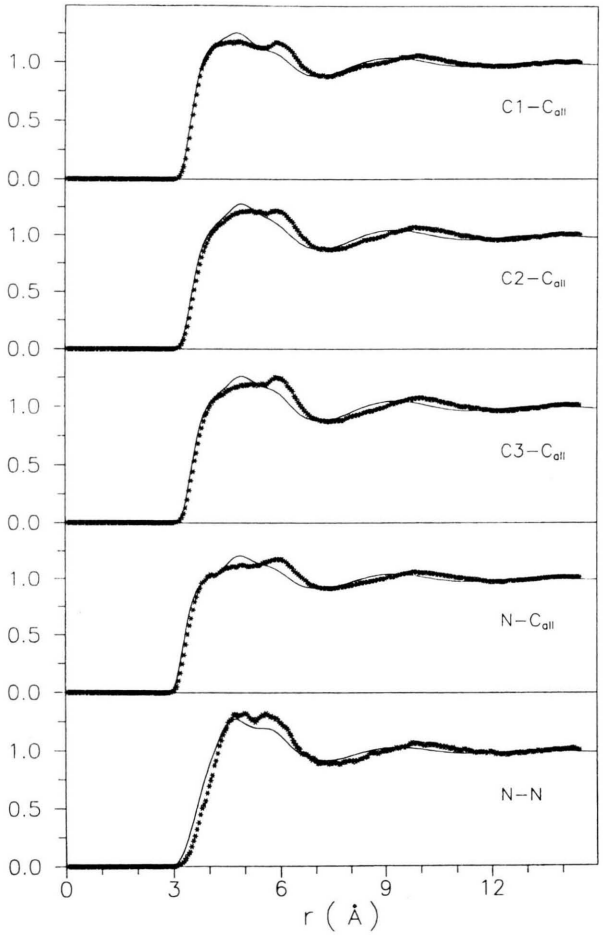

Fig. 2. Partial radial distribution functions from MD simulation (solid lines) and RISM theory (asterisks).

the N–N RDF. The reason for the shoulder or second peak in the C1–C_{all}, C2–C_{all}, C3–C_{all} and N–C_{all} partial pair distribution functions is the presence of two C1, C2 groups in every molecule. In all partial RDF'S the information is blurred, due to the large number of nearest neighbors, and therefore, it is not possible to separate a unique type of pair-interaction which mainly determines the structure of liquid pyridine.

The center of molecular mass radial distribution function is shown for liquid pyridine in Figure 3. The main peak of this function is found at about 5.6–5.8 Å, and integration to the minimum at 7.2 Å yields 13 molecules. The same coordination number has been found by experimental studies in the pyridine crystal [7].

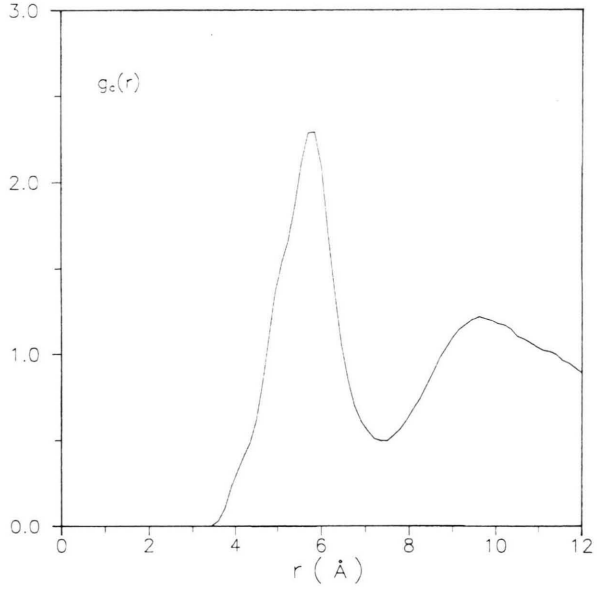

Fig. 3. Centre of mass radial distribution function for liquid pyridine, computed from MD simulation.

2.1.2 X-ray Structure Function

The total X-ray structure function $I(s)$ is the weighted sum of the partial site-site structure functions [14]:

$$I(s) = \frac{\Sigma_{\alpha\beta}(2-\delta_{\alpha\beta})\, f_\alpha f_\beta x_\alpha x_\beta i_{\alpha\beta}(s)}{(\Sigma_\alpha x_\alpha f_\alpha(s))^2}, \qquad (3)$$

where $f_\alpha(s)$ is the scattering amplitude of the particle type α as a function of the scattering variable $s = 4\pi/\lambda \sin\theta$, λ the wavelength of the incident radiation, 2θ the scattering angle, x_α the atomic fraction of the α type sites, and $i_{\alpha\beta}(s)$ the partial structure function of α, β pairs.

The distinct RDF, $G_d(r)$, characteristic of the liquid structure and not including the intramolecular contributions, has been calculated from the structure function according to the equation

$$G_d(r) = 1 + \frac{1}{2\pi^2 \varrho r} \int s\, I(s) \sin(s r)\, \mathrm{d}r\,. \qquad (4)$$

The experimental and calculated $G_d(r)$ functions (derived from simulation results and RISM calculations) are compared in Figure 4. All qualitative features of the experimental curve are reproduced both by the MD and RISM calculations. A small dis-

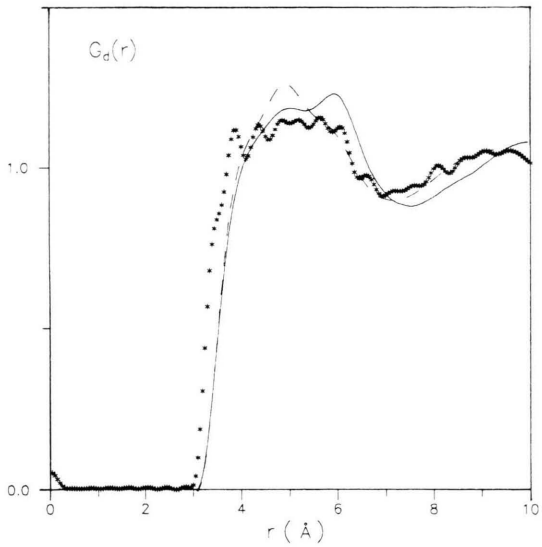

Fig. 4. Comparison of distinct radial distribution functions computed from MD simulation (solid line), RISM theory (dashed) and derived from the X-ray diffraction experiment (asterisks).

crepancy between the theoretical and experimental results can be seen at around 5–6 Å.

2.1.3 Orientational Correlation

In order to get more information regarding the orientational structure of liquid pyridine, two angular correlation functions were also computed. For this purpose, we considered the cosines

$$\cos \vartheta = \boldsymbol{a}_i \boldsymbol{a}_j , \tag{5}$$

$$\cos \varphi = \boldsymbol{n}_{ai} \boldsymbol{n}_{aj} , \tag{6}$$

$$\cos \alpha = \boldsymbol{n}_{ai} \boldsymbol{R}_{ij} , \tag{7}$$

$$\cos \beta = \boldsymbol{a}_i \boldsymbol{R}_{ij} , \tag{8}$$

where $\boldsymbol{a}_i$ and $\boldsymbol{n}_{ai}$ are unit vectors in the laboratory frame parallel to the dipole moment and perpendicular to the plane of the pyridine molecule, respectively; $\boldsymbol{R}_{ij}$ is a unit vector parallel to the vector between the molecular centres. By these definitions, the cosine distribution P of the angles ϑ and φ could be constructed as functions of the distance between the centres of mass. Here ϑ is the angle between the dipole moments of the central molecules and its neighbor, and φ is the angle between the planes of these molecules. Similarly, cosine distributions of the angles α and β could be constructed, where α is the angle between the normal vector of the first pyridine molecule and the distance vector between the centres of the two molecules, and β is the angle between the dipole vector of the first pyridine molecule and the distance vector between the centres of the two molecules.

Figure 5 shows the distribution of $\cos \vartheta$ and $\cos \varphi$ for various distance ranges between central and neighboring molecules: smaller than 4.5 Å, between 5.6 and 4.8 Å, between 4.8 and 5.6 Å, and between 5.6 and 7.2 Å. The corresponding coordination numbers are 1, 2, 6, and 13, respectively. For the first neighbors the distribution of $\cos \vartheta$ clearly shows a preference for antidipole orientation and the $\cos \varphi$ distribution demonstrates that the molecular planes of these molecules are almost parallel. The $\cos \alpha$ and $\cos \beta$ distributions reflect that the planes of the molecules do not coincide. These functions are shown in Figure 6. For distances larger than 5.6 Å, the $\cos \vartheta$ and $\cos \varphi$ functions show uniform distributions, witnessing a complete lack of preferred orientation.

2.2 *Dynamics*

Time dependence of the average motion of pyridine molecules can be followed through the translational and angular velocity autocorrelation functions, $\Phi_\alpha(t)$, $\Omega_\alpha(t)$, and the orientational correlation functions $C_l^\alpha(t)$, which are defined as

$$\Phi_\alpha(t) = \frac{\langle v_a(t)\, v_\alpha(0)\rangle}{\langle v_\alpha^2(0)\rangle} , \tag{9}$$

$$\Omega_\alpha(t) = \frac{\langle \omega_\alpha(t)\, \omega_\alpha(0)\rangle}{\langle \omega_\alpha^2(0)\rangle} , \tag{10}$$

and

$$C_l^\alpha(t) = \langle P_l \cos \Theta_\alpha(t)\rangle , \tag{11}$$

where $P_l \cos \theta_\alpha(t)$ is the l-th Legendre polynomial and $\theta_\alpha(t)$ is the angle through which a molecule fixed vector rotates in a time t; v_α and ω_α denote the center of mass and angular velocity of a particle α, respectively.

2.2.1 Translational Motion

In a molecular dynamics simulation the self diffusion coefficient can be readily calculated from MD simulation data by using Einstein's relation. It can also be obtained from the integral of the center of mass's velocity autocorrelation function. The two

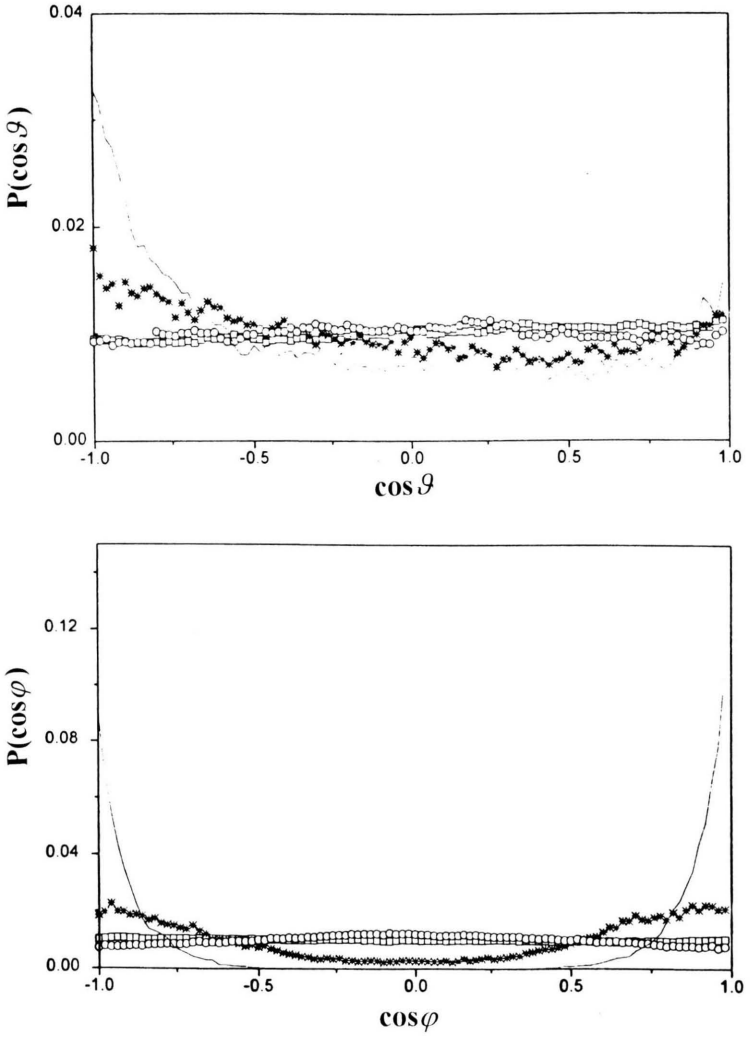

Fig. 5. Distribution of the cosine of the angles ϑ and φ (where ϑ is angle between the dipole vectors of two pyridine molecules and φ is the angle between the normal vectors of the planes of two pyridine molecules) in various distance ranges of the centres of mass, computed from MD simulation (solid: $r_c < 4.5$ Å, stars: 4.5 Å $< r_c < 4.8$ Å, circles: 4.8 Å $< r_c < 5.6$ Å, squares: 5.6 Å $< r_c < 7.2$ Å).

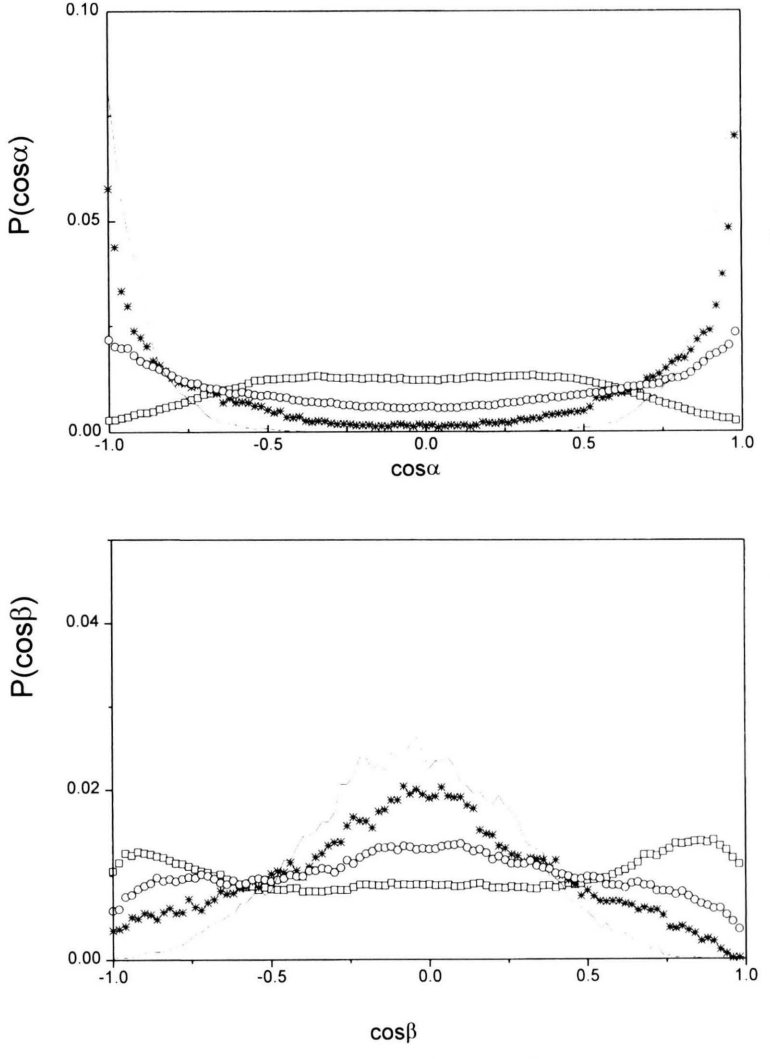

Fig. 6. Distribution of the cosine of the angles α and β (where α is angle between the normal vector of a pyridine molecule and the distance vector between the centres of two molecules and β is the angle between the dipole vector of a pyridine molecule and the distance vector between the centres of the two molecules) in various distance ranges of the centres of mass, computed from MD simulation (solid: $r_c < 4.5$ Å, stars: 4.5 Å $< r_c < 4.8$ Å, circles: 4.8 Å $< r_c < 5.6$ Å, squares: 5.6 Å $< r_c < 7.2$ Å).

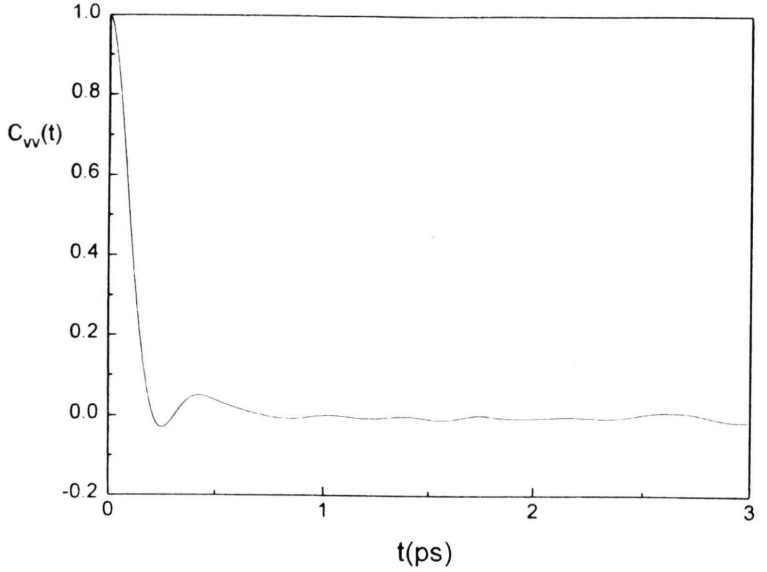

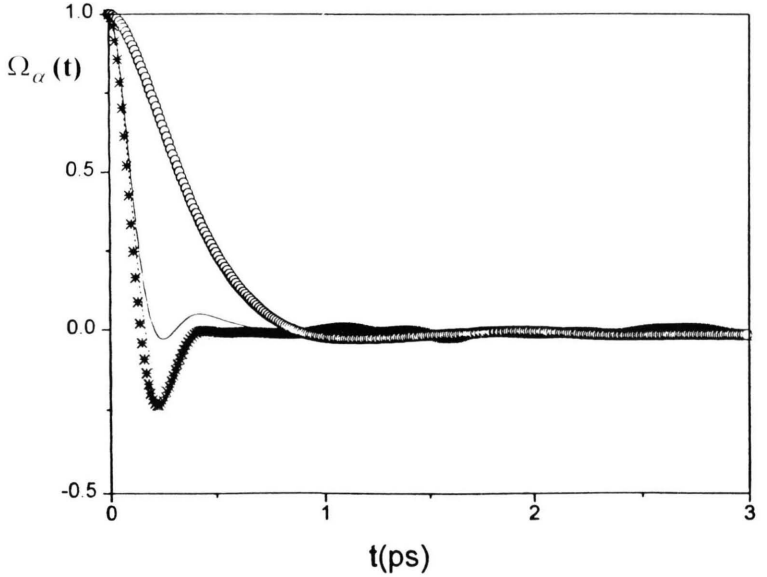

Fig. 7. a) Velocity autocorrelation function for liquid pyridine at 295 K. b) Angular velocity autocorrelation function and its decomposition into components directed along the principal axes (X, Y axes in the molecular plane and Z axis perpendicular to the lane of the molecule, (solid: total, dashed: X, stars: Y, circles: Z)).

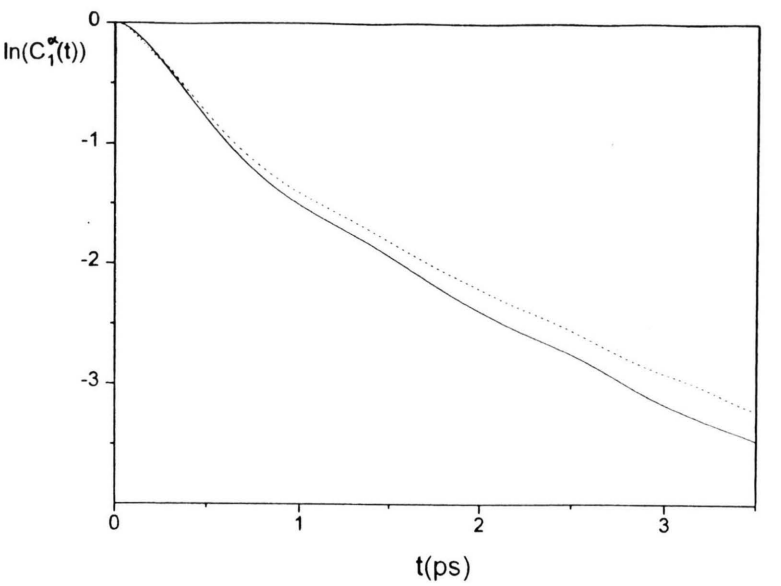

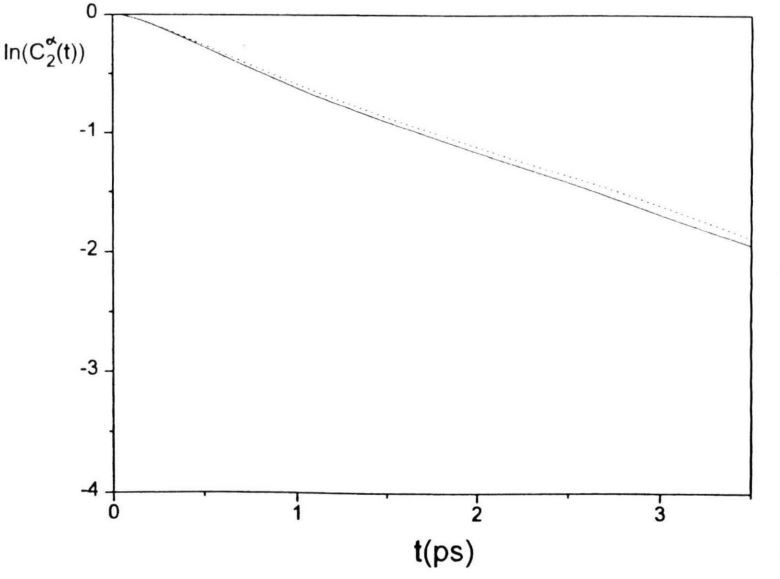

Fig. 8. Reorientational correlation functions $\ln C_1^\alpha(t)$ and $\ln C_2^\alpha(t)$ for different principal axes of liquid pyridine (solid: X, dashed: Y, dotted: Z).

routes give virtually the same result within the numerical accuracy. The self diffusion coefficient is found to be $D_s = 1.85 \times 10^{-5}$ cm^2/s. Unfortunately we could not compare our theoretical value with experimental ones, since there are none. Our theoretical value is slightly lower than the experimental value of liquid benzene [17] at 305 K ($D_s = 2.4 \times 10^{-5}$ cm^2/s). The normalised center of mass velocity autocorrelation function for liquid pyridine is shown in Figure 7a. It displays a negative region, which is often explained by the "cage effect" in liquids. A small double minimum is also exhibited, which was already found for liquid benzene, fluorine and chlorine. The autocorrelation function is probably dominated by noise in the time range above 2 ps.

2.2.2 Rotational Motion

The principal component of the angular velocity and the total angular velocity autocorrelation functions were calculated according to (10) and are shown in Figure 7b. The single molecule correlation times have been obtained by integrating the appropriate orientational correlation function according to

$$\tau_\alpha = \int \Omega_\alpha(t)\,\mathrm{d}t\,. \tag{12}$$

The components directed along the principal axes can be separated from the MD simulation. An appropriate choice for the definition of the molecular frame is to direct the Z axis perpendicular to the plane of the molecule. The characteristic times of rotational motion are shown in Table 1. A comparison between the experimental and the simulated rotational correlation times is also included. By this selection it can be observed that, although the time dependence of the characteristic times of rotational motions are different for each principal axis, those corresponding to the two axes within the plane of the molecule are almost equal. These results suggest that a "motional anisotropy" is present in liquid pyridine, a fact in good agreement with experimental observations [18].

The calculated ratio of the correlation times for rotation around the axis perpendicular to the molecular plane and around the axes within the plane is about 6.6.

2.2.3 Reorientational Motion

The orientational correlation functions $C_l^\alpha(t)$ are shown in Figure 8. These functions provide information about the orientational motion of the molecular principal axes. The function $C_l^\alpha(t)$ contains information which can be compared with the dielectric relaxation data for $l = 1$ and with NMR or NQR measurements for $l = 2$. At long times, all functions display the usual exponential decay.

Table 1. Characteristic times of rotational motions are compared: data calculated for the principal axes from MD simulation and those obtained from experiment [17]. X, Y and Z are the principal axes, $\parallel$ and $\perp$ denote rotations around axes parallel and perpendicular to the molecular plane respectively.

Total	X	Y	Z	$\parallel$ (exp.)	$\perp$ (exp.)
0.1 ps	0.05 ps	0.045 ps	0.33 ps	0.1 ps	0.04 ps

Table 2. Reorientational correlation times for liquid pyridine obtained from the MD simulation, compared with the experimental data. X and Y are the principal axes parallel to the molecular plane and Z is the one perpendicular to it.

	X	Y	Z	Exp.	Ref.
τ_1	2.04 ps	1.88 ps	4.16 ps	3.7–6.8 ps	[20]
τ_2	1.42 ps	1.2 ps	2.04 ps	1.4–2.3 ps	[18, 19]

In Table 2 results obtained for the correlation times are listed, according to (12) for τ_1 and τ_2, respectively. The appropriate tail corrections to the self times were added by assuming an exponential decay in $C_l^\alpha(t)$ at long times. The agreement in τ_2 is good, and in τ_1 the observable deviation is slight.

Kintzinger and Lehn found that the molecular motions are quite anisotropic and the molecular rotation about the axis perpendicular to the molecular plane is faster than the motion around the axes within the plane [19]. Schweitzer et al. showed, from ^{15}N NMR experiment, that the anisotropy of the motion is small [20].

If we consider that the molecular reorientational motion is anisotropic, reorientations of the X and Y axes become faster than the reorientation of the Z axis. The correlation times for the reorientational motion around the X and Y axes are nearly the same. The ratio of $\tau_{2x}/\tau_{2z} = 0.7$ shows a gas like motional anisotropy. It is important to note that this ratio is consistent with experiment [20] and simulation.

Our model shows that the molecular motions cannot be described as a rotational diffusion process, where the condition of $\tau_1/\tau_2 = 3$ should be valid.

3. Summary and Conclusion

In the present study we have shown, that the six center 12-6-1 OPLS potential allows a good qualitative description of the structure of liquid pyridine. The partial radial distribution functions computed from MD simulation and RISM calculation agree well with each other, which shows the applicability of RISM theory for liquid pyridine. The dipole-dipole interaction plays a significant role in forming the local structure in a short range around the central molecules and yields a preferred antidipole orientation. The calculated internal energy agrees well with experiment, and the simulation shows differences in the rotational motion around the axes within the plane of the molecule and perpendicular to it, with good agreement with experiment.

Acknowledgements

The authors are indebted to Dr. P. Bopp for his valuable discussions. The authors are also grateful to P. A. Monson for providing the RISM code. Financial support of the Hungarian OTKA Foundation (1807) is acknowledged.

[1] D. J. Evans and R. O. Watts, Mol. Phys. **32,** 93 (1976).
[2] G. Cicotti, M. Ferrario, and J. P. Ryckaert, Mol. Phys. **47,** 1253 (1982).
[3] F. Semano Adam, A. Banon, and J. Santana, Chem. Phys. **86,** 433 (1984).
[4] P. Linse, S. Engström, and B. Jönsson, Chem. Phys. Letter **115,** 95 (1985).
[5] W. L. Jorgensen and D. L. Severance, J. Am. Chem. Soc. **112,** 4768 (1990).
[6] O. Steinhauser, Chem. Phys. **73,** 155 (1982).
[7] Z. Gamba and M. L. Klein, Chem. Phys. **130,** 15 (1989).
[8] H. Bertagnolli, T. Engelhardt, and P. Chieux, Ber. Bunsenges. Phys. Chem. **90,** 512 (1986).
[9] T. Radnai, I. Bakó, P. Jedlovszky, and G. Pálinkás, Mol. Sim. **16,** 345 (1996).
[10] W. L. Jorgensen, J. M. Briggs, and M. L. Conteras, J. Phys. Chem. **94,** 1683 (1990).
[11] W. Smith, CCP5 Newsletter **7,** 5 (1982).
[12] B. M. Pettit and P. J. Rossky, J. Chem. Phys. **78,** 729 (1983).
[13] P. A. Monson, Mol. Phys. **47,** 435 (1982).
[14] G. Pálinkás, T. Radnai, and F. Hajdu, Z. Naturforsch. **35a,** 107 (1980).
[15] C. E. Bacon, N. A. Curry, and S. A. Willson, Proc. Roy. Soc. London **A279,** 98 (1964).
[16] D. Mootz and H. G. Wussow, J. Chem. Phys. **75,** 1517 (1981).
[17] M. A. McCool, A. F. Collingg, and L. A. Wolf, J. Chem. Soc. Faraday I **68,** 1489 (1972).
[18] B. Stryczek, J. Mol. Struct. **143,** 297 (1986).
[19] J. P. Kintzinger and J. M. Lehn, Mol. Phys. **22,** 273 (1971).
[20] D. Schweitzer and H. W. Spiess, J. Mag. Res. **15,** 529 (1974).
[21] R. A. Assink, J. DeZwaak, and J. Jonas, J. Chem. Phys. **56,** 4975 (1971).